Inorganic Chemistry

Article

pubs.acs.org/IC

Complexes of Lanthanide Nitrates with Tri Tert Butylphosphine Oxide

Allen Bowden,[†] Simon J. Coles,[‡] Mateusz B. Pitak,[‡] and Andrew W. G. Platt*[,§]

[†]Department of Chemistry and Analytical Sciences, The Open University, Walton Hall, Milton Keynes, MK7 6BT, U.K.

[‡]School of Chemistry, University of Southampton, Highfield Campus, Southampton, SO17 1BJ, U.K.

[§]Faculty of Sciences, Staffordshire University, College Road, Stoke-on-Trent, ST4 2DE, U.K.

Supporting Information

ABSTRACT: Reaction of lanthanide nitrates with $^{t}Bu_3PO$ (=L) lead to the isolation of complexes $Ln(NO_3)_3L_2{\cdot}H_2O{\cdot}n$EtOH (Ln = La (**1**), Nd(**2**)), $Ln(NO_3)_3L_2{\cdot}n$EtOH (Sm(**3**), Eu(**4**)), and $Ln(NO_3)_3L_2$ (Dy(**5**), Er(**6**), Lu(**7**)). These have been characterized by elemental analysis, infrared and NMR(^{1}H, ^{13}C and ^{31}P) spectroscopy and single-crystal X-ray diffraction. The structures show L to be positioned on opposite sides of the metal with the nitrates forming an equatorial band. When Ln = Dy, Er, and Lu two distinct molecules are present in the unit cell. A major isomer (70%) has a (P)O−Ln−O(P) angle of less than 180° with one of the nitrate ligands twisted out of the plane of the other nitrates while the lower abundance isomer is more symmetric with the (P)O−Ln−O(P) angle of 180° and the nitrate ligands coplanar giving a hexagonal bipyramidal geometry. These isomers cannot be observed by variable temperature solution ^{31}P NMR measurements but are clearly seen in the solid-state NMR spectrum of the Lu complex. Variable temperature solid-state NMR indicates that the isomers do not interconvert at temperatures up to 100 °C. Attempts to prepare cationic species $[Ln(NO_3)_2L_3]^{+}[PF_6]^{-}$ have not been totally successful and led to the isolation of crystals of $Lu(NO_3)_3L_2$ and $Tb(NO_3)_3L_2.CH_3CN$ (**8**).

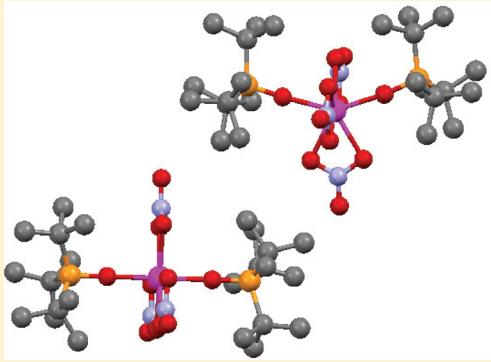

INTRODUCTION

Complexes between lanthanide nitrates and phosphine oxides have a long pedigree, with complexes of triphenylphosphine oxide in particular being extensively studied.[1−4]

Trialkylphosphine oxide complexes have received less attention. The complexes $Nd(NO_3)_3(R_3PO)_3$ (R = Me, Et)[5] were characterized by elemental analysis, infrared, and electronic spectroscopy. More extensive studies of the lanthanide series similarly revealed that the 1:3 composition $Ln(NO_3)_3(R_3PO)_3$ (R = butyl, octyl) is common[6] and $Am(NO_3)_3(R_3PO)_3$ and $Cm(NO_3)_3(R_3PO)_3$ were also deduced to have been formed in the solvent extraction with Bu_3PO and Oct_3PO.[7] The main technological interest in these complexes stems from their potential application in nuclear fuels reprocessing where the chemically robust nature of phosphine oxides is advantageous. In addition, there has been considerable research aimed at optimizing the solvent extraction properties of phosphine oxides by altering their peripheral structure.[8−13] Mixed trialkylphosphine oxides R_3PO (R = hexyl, heptyl, and octyl) have been used as extractants for lanthanide ions either alone[14,15] or in synergy with alkylphosphinic acids.[16]

We have previously examined the formation and properties of lanthanide nitrate complexes with R_3PO (R = cyclohexyl,[17] $^{i}Bu_3PO$[18]) and find that the structural theme for these complexes is $Ln(NO_3)_3(R_3PO)_3$ as expected, with subtle variations in structure as the ionic radius decreases.

We report here the extension of this study to the more sterically demanding $^{t}Bu_3PO$.

RESULTS AND DISCUSSION

The reactions of lanthanide nitrates with $^{t}Bu_3PO$ (=L) in a 1:3 ratio in ethanol led to the formation of complexes with a 1:2 metal to ligand ratio Ln = La(**1**), Nd(**2**), Sm(**3**), Eu(**4**), Dy(**5**), Er(**6**), Lu(**7**). The complexes of the heavier lanthanides were less soluble and crystallized readily from the reaction mixture. For the lighter metals (La and Nd) spontaneous crystallization did not occur on reducing the volume of ethanol and cooling the solutions. For these complexes, seeding the concentrated solutions with the solid obtained from evaporating a small amount of the solution was successful in giving crystalline complexes. Crystals of the lighter metals (La − Eu) deteriorate on exposure to the laboratory atmosphere due to loss of ethanol (see crystal structures), and have a bulk composition corresponding to $Ln(NO_3)_3L_2{\cdot}H_2O$. The complexes of the heavier lanthanides Dy − Lu, crystallized as $Ln(NO_3)_3L_2$, which are stable under ambient conditions. In contrast to reactions with less sterically demanding phosphine oxides, in no cases could we isolate neutral complexes with a 1:3 metal to ligand ratio under these conditions.

Received: January 19, 2012
Published: March 13, 2012

   dx.doi.org/10.1021/ic300142r | Inorg. Chem. 2012, 51, 4379−4389

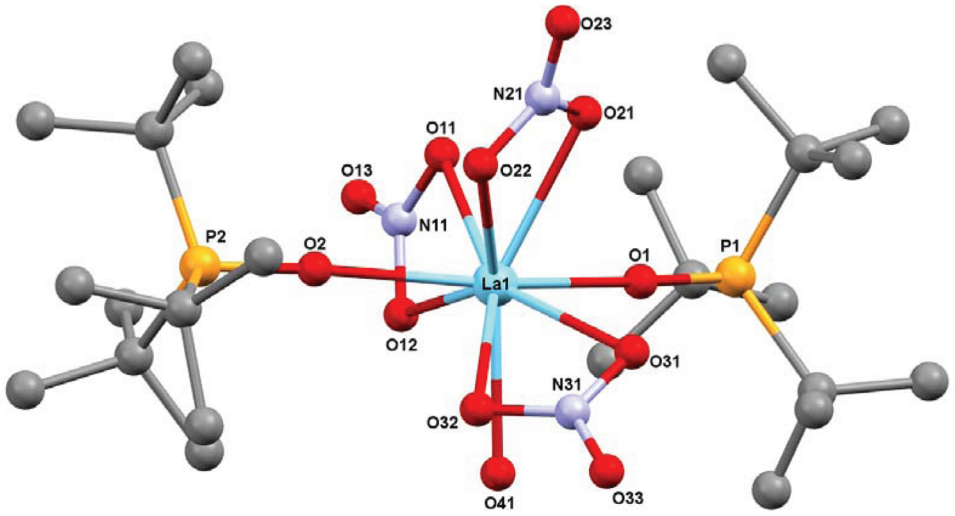

Figure 1. Molecular structure of $La(NO_3)_3(^tBu_3PO)_2{\cdot}H_2O{\cdot}2EtOH$ (**1**) (H atoms and the lattice ethanol molecules have been omitted for clarity).

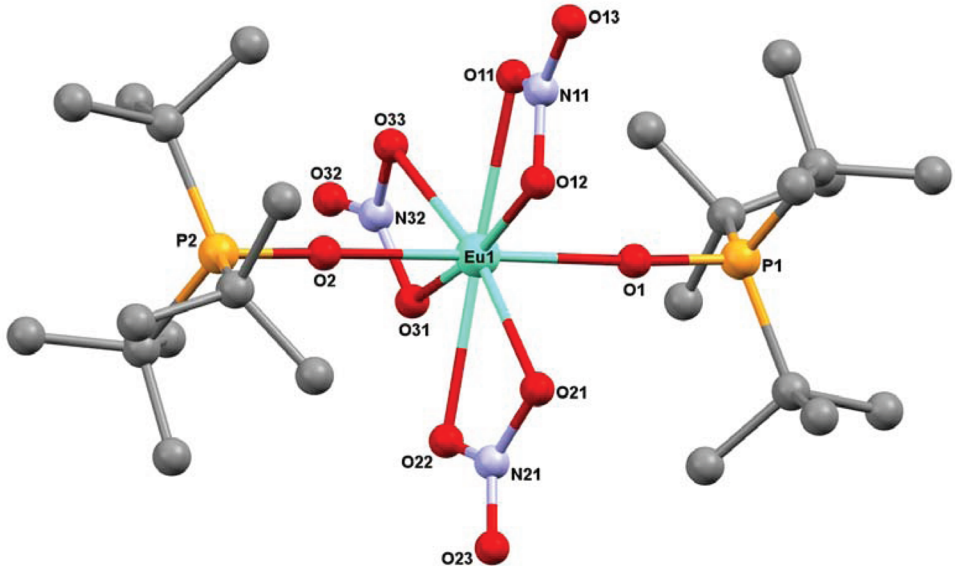

Figure 2. Molecular structure of $Eu(NO_3)_3(^tBu_3PO)_2{\cdot}EtOH$ (**4**). (H atoms and the lattice ethanol molecules have been omitted for clarity).

The X-ray crystal structures show interesting transitions from La to Lu. Nine-coordinate species $Ln(NO_3)_3L_2(H_2O){\cdot}2EtOH$ (Ln = La, Nd) form for the larger ions, whereas 8-coordinate complexes $Ln(NO_3)_3L_2{\cdot}x$EtOH where the ethanol is not directly bound to the metal, are found for Ln = Sm (x = 0.5) and Eu (x = 1). The ethanol molecules are not directly coordinated to the lanthanide ion in any of the complexes. The unsolvated complexes $Ln(NO_3)_3L_2$ are obtained for Ln = Dy, Er, Lu. The structures of each type of complex are shown in Figures 1−3 respectively. Details of the data collection and refinement for these complexes and $Tb(NO_3)_3L_2{\cdot}0.5CH_3CN$ are given in Tables 1a and 1b and selected bond distances in Table 2. The crystal structures are all similar in that the $^tBu_3PO$ ligands lie on opposite sides of the lanthanide ion in an axial arrangement, as would be expected on steric grounds, with the bidentate nitrates occupying an equatorial belt. The lanthanide ions lie close to the N3 plane in all cases, the greatest deviation being for the Eu complex where the metal ion is situated 0.188 Å from the plane. The nitrates generally have a puckered arrangement of their oxygen atoms relative to the N3 plane. The degree of puckering can be gauged in the average O···N3 plane distances. These distances average from 0.712 Å (range 0.158−1.029 Å) (La, Nd) reducing to about 0.2 Å (Sm, Eu). The Dy, Er, and Lu complexes exist as two isomers, with a lower abundance (30%) form having a highly symmetric structure (local C_{3v} symmetry) with the nitrates adopting a planar arrangement (maximum deviation of O from the N3 plane of 0.063 Å). In the higher abundance (70%) isomer one of the nitrate ligands is twisted with its oxygen atoms at approximately 90° to the N3 plane. The (P)O−Ln−O(P) angle varies with the size of the lanthanide ion. For the larger ions (La, Nd) this angle is bent significantly from linearity at 151.9°, whereas for the smaller Sm and Eu it is almost linear at about 177°. These changes are accompanied by the reduction in the puckering of the nitrate ligands described above. The low abundance isomers of the Dy − Lu complexes have a linear (P)O−Ln−O(P) geometry, whereas the twisting of the nitrate out of plane in the more abundant form induces a bending of this angle to minimize the unfavorable steric interactions.

The Ln−O distances for both nitrate and phosphine oxide show an approximately linear decrease with atomic number of

dx.doi.org/10.1021/ic300142r | Inorg. Chem. 2012, 51, 4379−4389

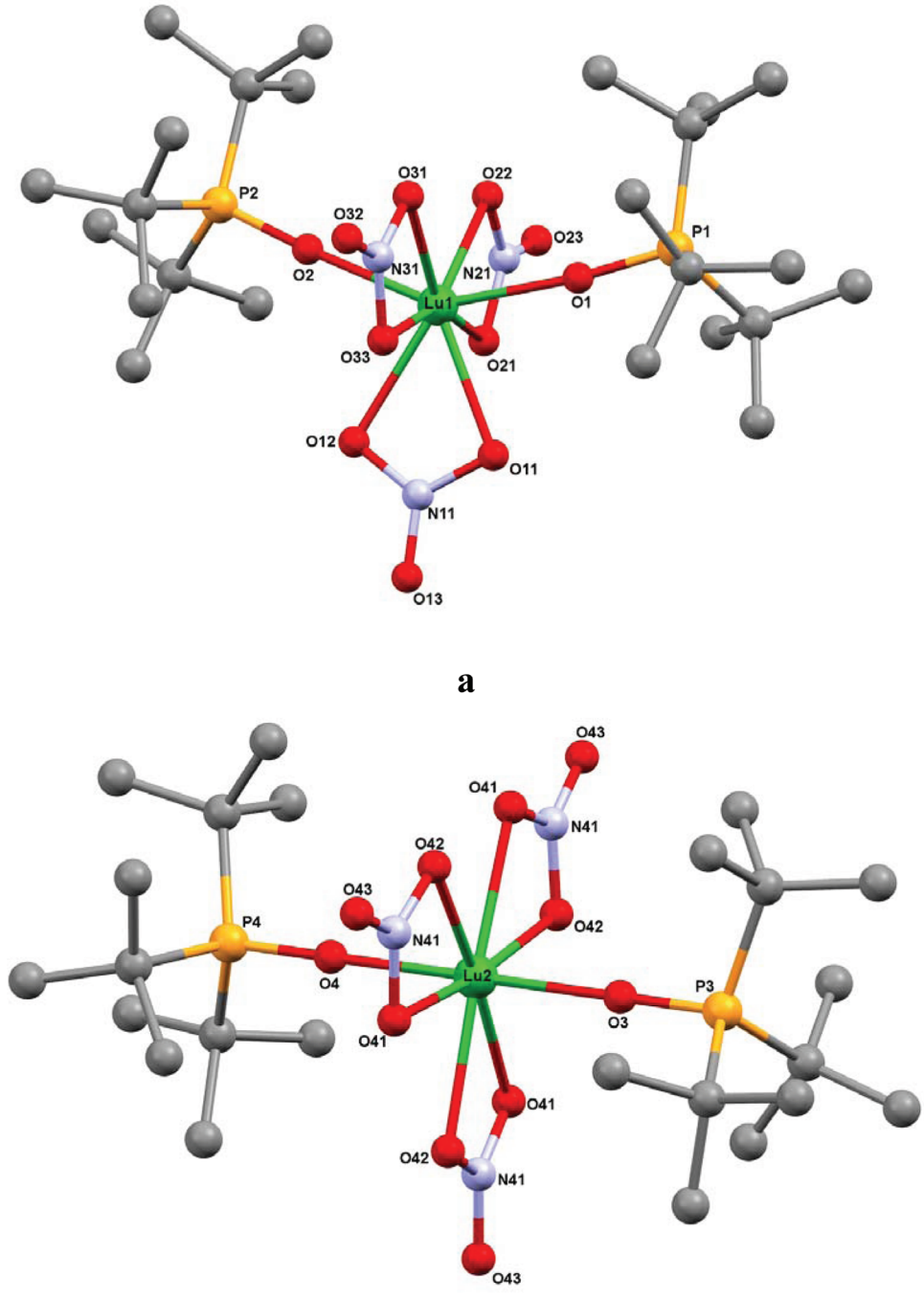

Figure 3. Molecular structures of the two isomers of $Lu(NO_3)_3(^tBu_3PO)_2$ (7); **a**) the 70% isomer, **b**) the 30% isomer (H atoms have been omitted for clarity).

the lanthanide, as expected from the lanthanide contraction. When these distances are corrected for the effect of the lanthanide contraction by subtraction of the appropriate ionic radius the residual values are essentially constant. This implies that the changes in observed Ln−O distances are accountable entirely by the lanthanide contraction. This is summarized in Figure 4.

This was further confirmed by single factor ANOVA analysis over all the residual Ln-O distances described above where no statistically significant differences were observed.

In $Ln(NO_3)_3L_2(H_2O)\cdot 2EtOH$ (Ln = La, Nd) the metal is 9-coordinate bound to two phosphine oxides and three bidentate nitrate ligands with a water molecule completing the coordination sphere. The three nitrogen atoms and the oxygen atom of the coordinated water lie approximately in the same plane (the maximum deviation is for the oxygen, which is 0.093 Å from the mean plane) and these structures can be envisaged as somewhat distorted octahedra if the nitrates are considered as pseudomonodentate ligands.

dx.doi.org/10.1021/ic300142r | *Inorg. Chem.* 2012, 51, 4379−4389

Table 1a. Data Collection and Refinement Details for (1)−(4)

empirical formula	$C_{28}H_{68}LaN_3O_{14}P_2$ (**1**)	$C_{28}H_{68}N_3NdO_{14}P_2$ (**2**)	$C_{50}H_{114}N_6O_{23}P_4Sm_2$ (**3**)	$C_{25}H_{57}EuN_3O_{11.50}P_2$ (**4**)
fw	871.7	877.03	1592.05	797.64
cryst syst	monoclinic	monoclinic	monoclinic	monoclinic
space group	$P2_1/n$	$P2_1/n$	$P2_1/c$	$C2/c$
unit cell dimensions Å	a = 17.3180(5) α = 90°	a = 17.2988(4) α = 90°	a = 13.7793(3) α = 90°	a = 19.2591(2) α = 90°
	b = 14.2982(5) β = 107.241(2)°	b = 14.2475(4) β = 107.2710(10)°	b = 16.6562(4) β = 93.2500(10)°	b = 27.2034(3) β = 93.8050(10)°
	c = 17.5534(6) γ = 90°	c = 17.4277(4) γ = 90°	c = 31.3629(7) γ = 90°	c = 13.8018(2) γ = 90°
volume Å^3	4151.2(2)	4101.64(18)	7186.5(3)	7215.00(15)
Z	4	4	4	8
density (calcd) Mg/m^3	1.395	1.42	1.471	1.469
absorption coefficient mm^{-1}	1.166	1.404	1.778	1.882
F(000)	1824	1836	3296	3304
temperature	153K	153K	153K	153K
crystal	block, colorless	block, colorless	block, colorless	prism, colorless
crystal size mm^3	0.12 × 0.12 × 0.04	0.12 × 0.10 × 0.10	0.08 × 0.06 × 0.05	0.12 × 0.07 × 0.06
θ range for data collection	3.46−27.48°	2.91−27.48°	2.91−27.50°	2.92−27.48°
index ranges	$-22 \le h \le 22$	$-22 \le h \le 22$	$-17 \le h \le 17$	$-24 \le h \le 25$
	$-18 \le k \le 18$	$-17 \le k \le 18$	$-21 \le k \le 20$	$-35 \le k \le 34$
	$-22 \le l \le 22$	$-22 \le l \le 22$	$-40 \le l \le 40$	$-17 \le l \le 17$
reflns collected	50 789	37 716	48 932	39 965
independent reflns	9504 [R_{int} = 0.0827]	9345 [R_{int} = 0.0362]	16358 [R_{int} = 0.0591]	8253 [R_{int} = 0.0402]
completeness to θ = 27.48°	99.70%	99.20%	99.10%	99.70%
max. and min transmission	0.9549 and 0.8728	0.8723 and 0.8496	0.9163 and 0.8708	0.8954 and 0.8056
data/restraints/params	9504/3/461	9345/3/461	16358/0/804	8253/2/401
GOF on F^2	1.038	1.096	1.126	1.078
final R indices [$F^2 > 2s(F^2)$]	$R1$ = 0.0476, wR2 = 0.1022	$R1$ = 0.0322, wR2 = 0.0656	$R1$ = 0.0544, wR2 = 0.1071	$R1$ = 0.0278, wR2 = 0.0585
R indices (all data)	$R1$ = 0.0696, wR2 = 0.1114	$R1$ = 0.0412, wR2 = 0.0709	$R1$ = 0.0734, wR2 = 0.1179	$R1$ = 0.0331, wR2 = 0.0618
largest diff. peak and hole eÅ^{-3}	1.774 and −1.237	1.164 and −0.632	0.962 and −0.640	0.560 and −0.749

dx.doi.org/10.1021/ic300142r | *Inorg. Chem.* 2012, 51, 4379−4389

Table 1b. Data Collection and Refinement Details for (5)−(8)

empirical formula	$C_{24}H_{54}DyN_3O_{11}P_2$ (5)	$C_{32}H_{72}Er_{1.33}N_4O_{14.67}P_{2.67}$ (6)	$C_{32}H_{72}Lu_{1.33}N_4O_{14.67}P_{2.67}$ (7)	$C_{33.33}H_{74}N_{4.67}O_{14.67}P_{2.67}Tb_{1.33}$ (8)
fw	785.14	1053.2	1063.48	1069.45
cryst syst	trigonal	trigonal	trigonal	monoclinic
space group	*R*3	*R*3	*R*3	$P2_1/c$
unit cell dimensions Å	a = 28.2470(3) Å α = 90°	a = 28.2812(4) α = 90°	a = 28.2896(4) α = 90°	a = 13.7432(13) Å α = 90°
	b = 28.2470(3) Å β = 90°	b = 28.2812(4) β = 90°	b = 28.2896(4) β = 90°	b = 16.6395(16) Å β = 92.244(2)°
	c = 15.0660(3) Å γ = 120°	c = 15.0594(4) γ = 120°	c = 15.0017(3) γ = 120°	c = 31.248(3) Å γ = 90°
volume Å^3	10410.5(3) Å^3	10431.2(3)	10397.4(3)	7140.3(12) Å^3
Z	12	9	9	6
density (calculated) Mg/m^3	1.503 Mg/m^3	1.509	1.529	1.492 Mg/m^3
absorption coefficient mm^{-1}	2.299 mm^{-1}	2.559	2.995	2.125 mm^{-1}
F(000)	4836	4860	4896	3304
temp	153K	153K	153K	153K
crystal	block, colorless	block, colorless	block, colorless	prism, colorless
cryst size mm^3	0.14 × 0.03 × 0.02	0.18 × 0.13 × 0.08	0.35 × 0.30 × 0.22	0.08 × 0.06 × 0.05 mm^3
θ range for data collection	3.18−27.48°	3.18−27.50°	3.18−27.48°	2.92−27.50°
index ranges	$-36 \le h \le 36$	$-36 \le h \le 36$	$-25 \le h \le 33$	$-17 \le h \le 17$
	$-36 \le k \le 29$	$-36 \le k \le 31$	$-36 \le k \le 36$	$-13 \le k \le 21$
	$-18 \le l \le 19$	$-19 \le l \le 19$	$-19 \le l \le 17$	$-40 \le l \le 36$
reflns collected	23 210	27 280	24 102	46 494
independent reflns	10 212 [R_{int} = 0.0633]	10 577 [R_{int} = 0.0466]	9628 [R_{int} = 0.0383]	16 204 [R_{int} = 0.0343]
completeness to θ = 27.48°	99.80%	99.70%	99.80%	98.90%
max. and min transmission	0.9555 and 0.7390	0.8215 and 0.6559	0.5587 and 0.4204	0.9012 and 0.8484
data/restraints/params	10 212/1/518	10 577/1/518	9628/1/520	16 204/0/788
GOF on F^2	1.116	1.022	1.035	1.06
final R indices [$F^2 > 2\sigma(F^2)$]	$R1$ = 0.0491, wR2 = 0.0944	$R1$ = 0.0324, wR2 = 0.0566	$R1$ = 0.0225, wR2 = 0.0431	$R1$ = 0.0329, wR2 = 0.0644
R indices (all data)	$R1$ = 0.0589, wR2 = 0.1006	$R1$ = 0.0379, wR2 = 0.0587	$R1$ = 0.0232, wR2 = 0.0433	$R1$ = 0.0372, wR2 = 0.0664
largest diff. peak and hole eÅ^{-3}	1.364 and −0.637	1.008 and −0.854	0.579 and −0.705	1.062 and −0.807 e Å^{-3}

dx.doi.org/10.1021/ic300142r | *Inorg. Chem.* 2012, 51, 4379−4389

Table 2. Selected Bond Distances /Å in Compounds (1) to (8)

	La(1)	Nd(2)	Sm(3)	Eu(4)	Tb(8)	Dy(5)	Er(6)	Lu(7)
O1−Ln1	2.418(2)	2.3688(18)	2.255(3)	2.2438(16)	2.2145(19)	2.207(5)	2.206(3)	2.168(2)
O2−Ln1	2.396(2)	2.3451(18)	2.258(3)	2.2413(16)	2.2200(19)	2.212(5)	2.199(3)	2.176(2)
O3−Ln2			2.259(3)		2.2127(19)	2.193(9)	2.187(5)	2.159(4)
O4−Ln2			2.272(3)		2.2232(18)	2.206(8	2.196(5)	2.166(4)
O11−Ln1	2.633(2)	2.5660(19)	2.469(4)	2.4572(19)	2.436(2)	2.415(5)	2.385(3)	2.363(3)
O12−Ln1	2.616(3)	2.5559(19)	2.478(4)	2.456(2)	2.441(2)	2.416(5)	2.391(3)	2.363(3)
O21−Ln1	2.582(3)	2.527(2)	2.493(4)	2.4816(19)	2.454(2)	2.394(5)	2.367(3)	2.329(3)
O22−Ln1	2.633(3)	2.566(2)	2.481(4)	2.4885(19)	2.444(2)	2.453(5)	2.428(3)	2.397(3)
O31−Ln1	2.615(3)	2.548(2)	2.487(4)	2.4705(19)	2.452(2)	2.453(5)	2.434(3)	2.400(3)
O32−Ln1	2.653(2)	2.587(2)	2.488(4)	2.4815(19)	2.448(2)	2.418(5)	2.382(3)	2.341(3)
O41−Ln2			2.468(4)		2.423(2)	2.431(5)[a]	2.407(3)[a]	2.387(3)
O42−Ln2			2.469(4)		2.441(2)	2.445(5)[a]	2.417(3)[a]	2.397(3)
O51−Ln2			2.480(4)		2.459(2)			
O52−Ln2			2.486(4)		2.467(2)			
O61−Ln2			2.478(4)		2.447(2)			
O62−Ln2			2.495(4)		2.448(2)			
H_2O−Ln1	2.533(3)	2.475(2)						
O1−P1	1.523(2	1.520(2)	1.522(4)	1.5245(17)	1.522(2)	1.516(5)	1.508(3)	1.519(3)
O2−P2	1.521(3)	1.5184(19)	1.527(4)	1.5206(17)	1.526(2)	1.512(5)	1.518(3)	1.514(3)
O3−P3			1.516(4)		1.522(2)	1.530(10	1.531(6)	1.527(5)
O4−P4			1.518(3)		1.5267(19)			

Symmetry transformations used to generate equivalent atoms:

[a] $-x + y + 1, -x + 2, z$. [b] $-y + 2, x - y + 1, z$.

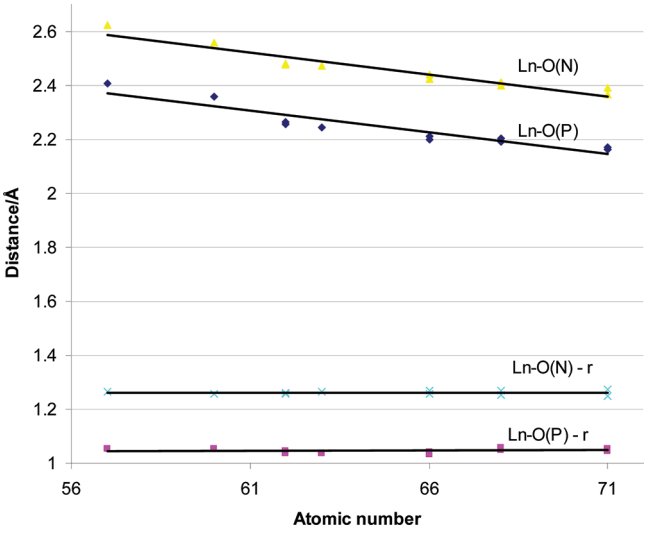

Figure 4. Ln−O distances and the distances corrected for the lanthanide contraction.

A network of hydrogen bonds involving the coordinated water molecules, nitrate ligands and noncoordinated ethanol molecules exists as shown in Figure 5. A dimeric unit is formed by H-bonding between the coordinated water molecules and the terminal oxygen of the nitrate on an adjacent molecule giving a 12-membered ring. An 8-membered ring is formed by H-bonding between the coordinated water, two lattice ethanol molecules and the O of a nitrate ligand. The O···O distances vary between 2.718−2.907 Å, which is within the range expected for hydrates.[19]

The solid-state ^{31}P and ^{15}N NMR spectra of $Lu(^{15}NO_3)_3L_2$ have been obtained over a range of temperatures and are shown in Figure 7. The ^{31}P spectra show the 4 signals expected from the crystallographically independent phosphorus atoms but with differing linewidths. Signals for the major isomer are assigned to peaks at 78.2 and 79.2 ppm, whereas those for the minor isomer are at 80.5 and 81.8 ppm. The integrated peak areas from the deconvoluted spectra vary depending on the temperature and probably are influenced by differing relaxation rates for the nuclei in different crystallographic environments. The ^{15}N spectra show two signals of differing line width at −7.5 ppm (sharp) and −9.6 ppm (broad). These are tentatively assigned to the nitrate twisted out of plane in the most abundant isomer and the in plane nitrates for both isomers, respectively. The sharp signal arises as there is only one crystallographic environment for this nitrate ligand, whereas the in plane nitrates have a total of three independent environments (two for the 70% isomer and one for the 30%) and would thus be expected to give broader signals. The ^{15}N spectra recorded with different contact times of 1, 3, and 5 ms are shown in the insert to part d of Figure 6 and show that the two signals have different cross-polarization behavior. Thus, the signal intensities do not necessarily relate directly to the abundance of the environments in the sample. There is no observable exchange between the phosphorus or nitrogen environments such as coalescence of signals on increasing the temperature to 100 °C. A ^{31}P EXSY experiment conducted at 100 °C did show low intensity cross peaks linking the two peaks for the major isomer. These could arise from chemical exchange or spin diffusion between the two environments in the major isomer. No such correlations are seen for the peaks in the minor isomer most probably as a result of the longer P···P distance and the lower intensity of the signals. It thus seems that in the solid state there is no interconversion of the isomers or a change in their relative abundance. The changes observed in the high-temperature NMR spectra are reversible and probably due to differing relaxation rates as a function of temperature.

dx.doi.org/10.1021/ic300142r | Inorg. Chem. 2012, 51, 4379−4389

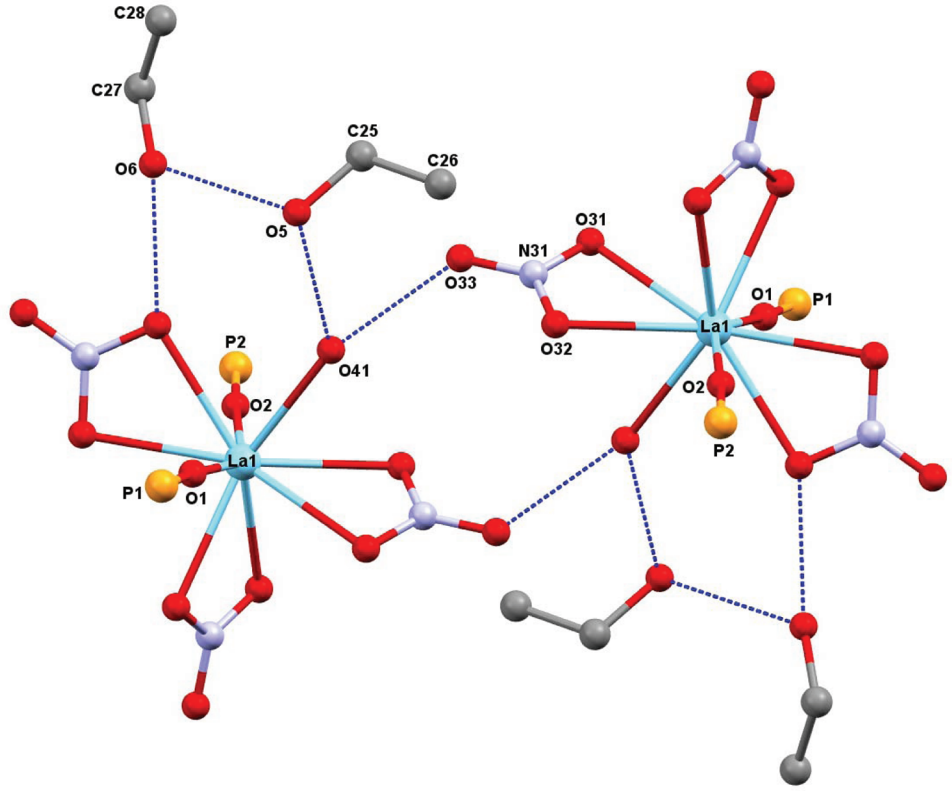

Figure 5. Hydrogen bonding network in $La(NO_3)_3(^tBu_3PO)_2H_2O{\cdot}2EtOH$ (**1**) (^{t}Bu groups and all hydrogen atoms have been omitted for clarity). O5–H5···O6^i = 2.727(4) Å, O6–H6···O12^{ii} = 2.838(4) Å, O41–H42···O33^{iii} = 2.907(4) Å, O41–H41···O5 = 2.718(4)2.718(4) Å; Symmetry transformations used to generate equivalent atoms: (i) $-x+{}^3/_2, y+{}^1/_2, -z+{}^3/_2$, (ii) $-x+{}^3/_2, y-{}^1/_2, -z+{}^3/_2$, (iii) $-x+1, -y+1, -z+2$.

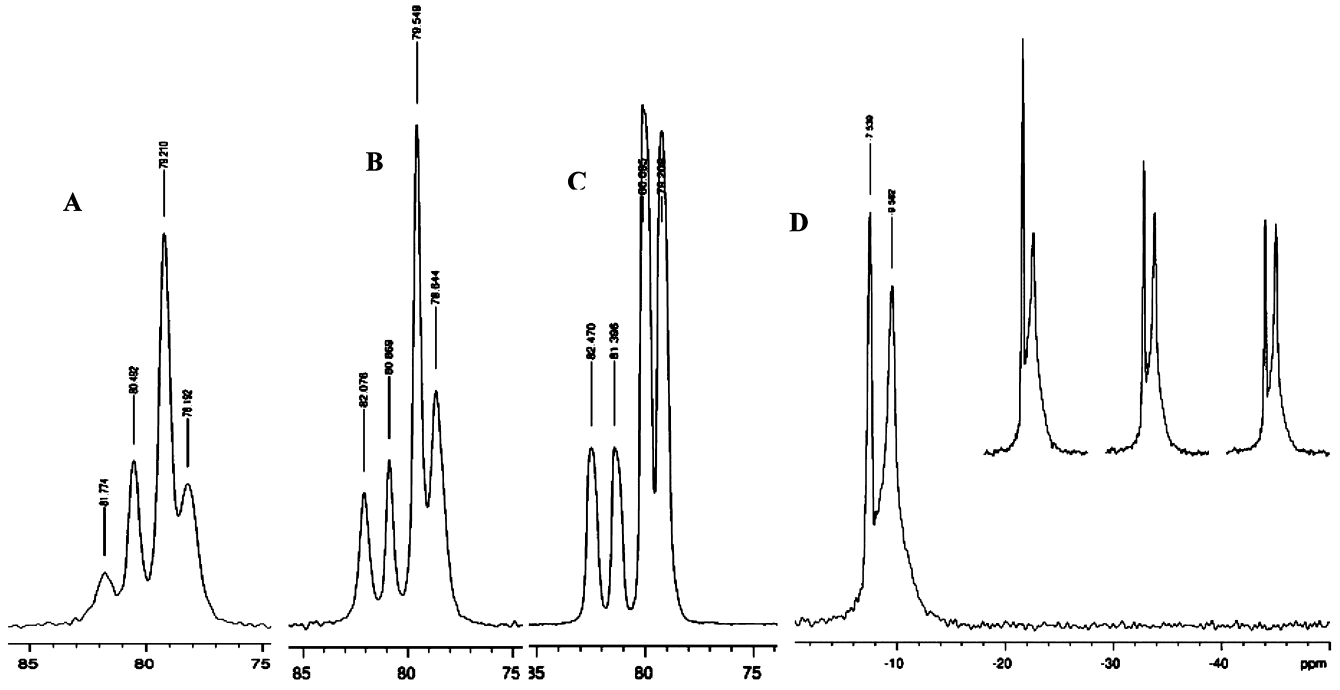

Figure 6. CPMAS ^{31}P and ^{15}N NMR spectra of $Lu(NO_3)_3(^tBu_3PO)^a$.
^{a}A ^{31}P at 25 °C, B ^{31}P at 50 °C, C ^{31}P at 100 °C, D ^{15}N at 25 °C (inset spectra recorded with 1, 3, and 5 ms contact time respectively).

In addition to single crystal X-ray diffraction, the complexes were characterized by elemental analyses, electrospray mass spectrometry, and solution NMR spectroscopy. The infrared spectra of the isolated solids show the expected bands with OH stretches between 3500–3300 cm^{-1} for complexes with lanthanide coordinated water (La, Nd) and lattice ethanol (Sm, Eu). Three bands typical of coordinated nitrate are seen as a series of absorptions between 1460 and 1444 (La) – 1512

dx.doi.org/10.1021/ic300142r | Inorg. Chem. 2012, 51, 4379–4389

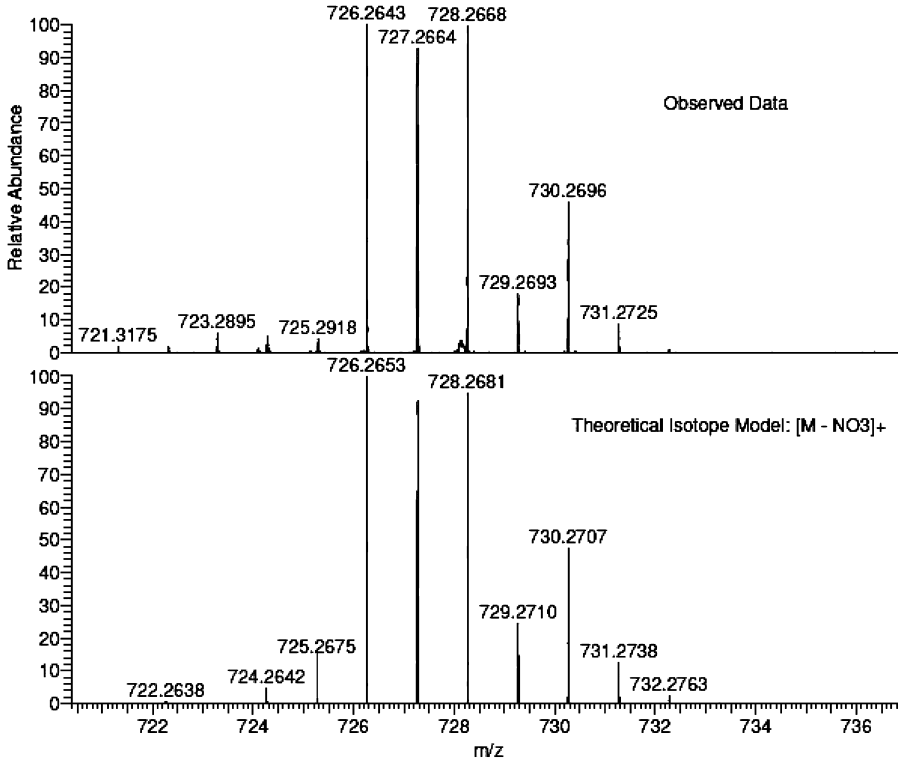

Figure 7. Observed and theoretical isotope profiles for $[Er(NO_3)_2L_2]^+$.

and 1471 cm^{-1} (Lu), and single peaks at 1300 (La) − 1280 cm^{-1} (Lu) and 1030 (La) − 1022 cm^{-1} (Lu), whereas the PO stretch is observed between 1065 cm^{-1}(La) and 1085 cm^{-1}(Lu) compared with 1107 cm^{-1} for the free ligand. The assignments were confirmed by the preparation of $Lu(^{15}NO_3)_3L_2$, which shows the N−O vibrations shifted to lower wavenumber particularly for the stretching modes as expected. Full infrared data and assignments are given in the Supporting Information. The electrospray mass spectra from dichloromethane/acetonitrile solution show that ligand redistribution occurs extensively during the electrospray process and it is interesting in this regard that $[Ln(NO_3)_2L_3]^+$ is always the most abundant lanthanide containing ion, with the expected parent ion $[Ln(NO_3)_2L_2]^+$ always present, but represented by a significantly lower intensity signal in all cases. The assignments are supported by the excellent agreement between observed and calculated m/z values (all within 10 ppm) and the match between the experimental and predicted isotope distribution profiles. An example for $[Er(NO_3)_2L_2]^+$ is shown in Figure 7. Full details of the spectra and the assignments are given in the Supporting Information.

Given the abundance of $[Ln(NO_3)_2L_3]^+$ in the mass spectra it seemed logical to attempt the synthesis of complexes containing this ion. The reaction of $Ln(NO_3)_3$ (Ln = Pr, Tb, and Lu) and three equivs of L with a suspension of KPF_6 in CH_3CN led to the isolation of crystalline materials which contained the $[PF_6]^-$ ion. The infrared spectra show strong bands at 790 and 550 cm^{-1} assigned to $[PF_6]^-$ and the ^{31}P NMR spectra show the expected binomial septet at about δ −144 ppm $^1J_{PF}$ = 707 Hz. The ^{31}P NMR spectra in CD_3CN also indicate that the isolated materials contain $Ln(NO_3)_3L_2$ and at least one other complex. At 80 °C the spectra of the solid from Lu reaction shows, in addition to $[PF_6]^-$, a single peak as a result of rapid exchange on the NMR time scale. On cooling, this band broadens and at −40 °C more complex spectra are observed with a sharp peak assignable to $Lu(NO_3)_3L_2$ at 79.7 ppm by comparison with the spectrum of a solution of an authentic sample in CD_2Cl_2, and also on the basis of the weighted average of the chemical shifts in the solid-state NMR spectrum (79.4 ppm) and other major signals at 77.9 (sharp) and 82.0 ppm (broad). Crystallization of the reaction mixtures yielded only $Lu(NO_3)_3L_2$ and $Tb(NO_3)_3L_2{\cdot}0.5CH_3CN$ (**8**) from the corresponding reaction with $Tb(NO_3)_3$. Here, it seems that the isolated mixture contains crystals of the $Ln(NO_3)_3L_2$ complexes with any cationic species being present as non crystalline material.

Solution structures and dynamics have been investigated in CD_2Cl_2 solution by multinuclear NMR spectroscopy. Full details of the NMR parameters are given in the Supporting Information and are as expected for the ligand coordinated to a lanthanide center. The ^{31}P NMR spectra generally show a single signal at 20 °C. On cooling the solutions the shifts of the paramagnetic complexes show a pronounced temperature dependence, particularly Dy for which the shift decreases by approximately 12 ppm/°C. At −90 °C the complexes of the lighter metals (La − Sm) show several additional low intensity signals which imply that a dynamic equilibrium exists between different structures in solution. The Eu − Lu complexes show a single resonance at all temperatures. This is despite the fact that in the solid state the complexes of Dy, Er, and Lu exist as two distinct isomers. Thus in CD_2Cl_2 it seems that either rapid exchange occurs between the two isomers or only one is present on dissolution and that in the solid state the two forms are of very similar energy and the isomers arise as a result of crystal packing effects.

Exchange between free and bound ligand was examined by addition of a small quantity of L to CD_2Cl_2 solutions of the complexes. For the complexes of La − Sm a single peak at an average position is observed at 20 °C, which is indicative of

dx.doi.org/10.1021/ic300142r | Inorg. Chem. 2012, 51, 4379−4389

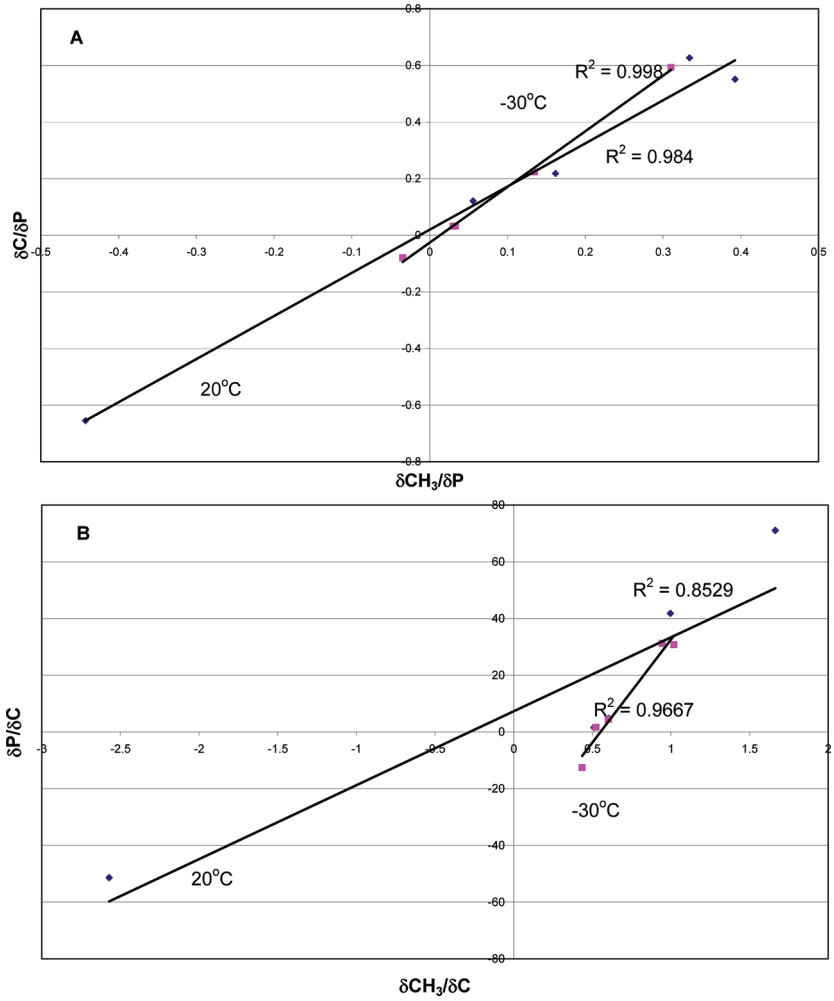

Figure 8. Shift ratio plots of A $\delta C/\delta P$ vs $\delta CH_3/\delta P$ and B $\delta P/\delta C$ vs $\delta CH_3/\delta C$ at 20 °C and −30 °C.

rapid exchange between free and bound ligand. At lower temperatures separate signals for free and bound ligand are observed in addition to other low intensity peaks. These are tentatively assigned to the presence of 1:3 complexes formed in solution, although we have not been able to isolate these species. For the complexes of the heavier metals exchange is slower at 20 °C and two broad signals are observed. This behavior is understandable on the basis that the ligands will be more tightly bound as a result of the higher charge density on the smaller ions toward the right of the lanthanide series.

The ^{13}C spectra show the expected features of the coordinated ligand with a doublet ($^1J_{PC}$~ 49 Hz) due to the $\underline{C}Me_3$ and a singlet due to the methyl groups. At low temperatures the signals from the CH_3 groups broaden and at −90 °C two separate peaks are observable, where the line width permits, in an approximately 2:1 ratio. This could possibly be due to restricted rotation of the ^{t}Bu groups leading to the inequivalence of the methyl groups, or the presence of other isomers in solution as indicated by the low-temperature ^{31}P NMR spectra. The ^1H NMR spectra were not easily interpretable for all the complexes. Where good spectra were obtained, La − Eu and Lu, the methyl signal in the ^1H NMR spectra broadens at −90 °C, but no further splitting was observed in any instance.

Analysis of lanthanide induced shifts has previously been used to deduce whether structures remain constant across the lanthanide series in solution. Analyses of shift ratio plots based on the observation of three nuclei[20,21] in a complex offer a model independent method of evaluating whether solution structures remain the same across a series, although the analysis is less sensitive to small structural changes. We have been able to observe the ^{31}P and two ^{13}C signals at 20 and −30 °C. The shift ratio plots are shown in Figure 8 indicate that there are no large changes in structure in solution. This, at first sight, might seem strange as the X-ray structures show clear differences. However as the solution NMR spectra show average structures and as the differences in the solid state structures are generally small it may well be that the shift ratio plots are not sufficiently sensitive to detect relatively small changes in the averaged structures.

■ CONCLUSIONS

The complexes of L = ^{t}Bu$_3$PO with lanthanide nitrates form $Ln(NO_3)_3L_2$ for all Ln studied in contrast to the $Ln(NO_3)_3(R_3PO)_3$ formulation found in other trialkylphosphine oxide complexes. This difference is readily explained by the steric requirements of the ligand. Attempts to observe in solution and isolate cationic species such as $[Ln(NO_3)_3L_3]^+$, which are clearly seen in the gas phase have given ambiguous results an no complexes which contain these cations have been prepared free from $Ln(NO_3)_3L_2$. While attempts to prepare pure samples containing $[Ln(NO_3)_2L_3]^+$ have not been successful, the preliminary results are encouraging and further work in this area is presently under

dx.doi.org/10.1021/ic300142r | Inorg. Chem. 2012, 51, 4379−4389

investigation particularly as the cone angle of $^{t}Bu_3PO$ is only 12° larger than that of Cy_3PO for which 1:3 complexes have been isolated.

EXPERIMENTAL SECTION

Crystallography. Suitable crystals were selected and single-crystal X-ray diffraction analyses were performed using a Bruker APEXII CCD diffractometer mounted at the window of a Bruker FR591 rotating anode (Mo Kα, λ = 0.71073 Å) and equipped with an Oxford Cryosystems Cryostream device at 120K. Data were processed using the *COLLECT* package[22] and unit cell parameters were refined against all data. An empirical absorption correction was carried out using SADABS.[23]

The crystal structure was solved by direct methods and full-matrix least-squares refinement on F_o^2 was carried out using SHELX-97 software package.[24] All non-hydrogen atoms were refined anisotropically, with all hydrogen atoms placed geometrically using standard riding models. All hydrogen atoms were added at calculated positions and refined using a riding model with isotropic displacement parameters based on the equivalent isotropic displacement parameter (Ueq) of the parent atom.

Crystal structures of (**4**) and (**8**) contain disordered solvent molecules. In (**4**) disordered ethanol was modeled over two positions with distance restraints (DFIX) used to maintain sensible C−C and C−O bond lengths and molecular geometry. In (**8**) the disordered acetonitrile molecule was located. The atomic displacement parameters were refined as isotropic only.

Crystal structures of (**5**), (**6**) and (**7**) have been refined as racemic twins in noncentrosymmetric spacegroup R3.

Crystallographic data (excluding structure factors) for the structures in this paper have been deposited with the Cambridge Crystallographic Data Centre as supplementary publication numbers CCDC 834847−834853 for compounds (**1**)−(**7**) and CCDC 857253 for (**8**).

Copies of the data can be obtained, free of charge, on application to CCDC, 12 Union Road, Cambridge CB2 1EZ, UK (Fax: +44(0)−1223−336033 or e-mail: deposit@ccdc.cam.ac.uk

Mass spectra were obtained on a Thermofisher LTQ Orbitrap XL at the EPSRC National Mass Spectrometry Service Centre at Swansea University. Samples (~10 mg) were dissolved in 300 μL CH_2Cl_2 and were loop injected into a stream of actetonitrile.

Infrared spectra were recorded with a resolution of ±2 cm^{-1}on a Thermo Nicolet Avatar 370 FTIR spectrometer operating in ATR mode. Samples were compressed onto the optical window and spectra recorded without further sample pretreatment.

NMR spectra were recorded on a JEOL EX 400 in CD_2Cl_2 solutions approximately 20 mg of complex dissolved in about 0.75 mL of solvent.

Synthesis. $^{t}Bu_3PO$: $^{t}Bu_3P$ (1.26 g 6.23 mmol) in 5 mL acetone was added to a stirred solution of H_2O_2 (0.82 g 30% aqueous solution) in 50 mL acetone. The temperature rose to 35 °C during the addition. The solution was stirred overnight and evaporated to dryness and the residue dried in vacuo over KOH to give 1.34 g of a waxy colorless solid. NMR (CD_2Cl_2) ^{31}P (161.8 MHz) δ 66.64, ^{13}C (100.5 MHz) $\underline{C}Me_3$ δ 39.32(d) $^{1}J_{CP}$ 50.7 Hz, Me δ 29.17 (s), ^{1}H (399.8 MHz) Me δ 1.36 (d) $^{3}J_{PH}$ 12.3 Hz.

$La(NO_3)_3(^{t}Bu_3PO)_2{\cdot}H_2O$: $La(NO_3)_36H_2O$ (0.10 g 0.22 mmol) in 1.0 g ethanol and $^{t}Bu_3PO$ (0.14 g 0.66 mmol) in 0.40 g ethanol were mixed and heated to 70 °C for 30 min. Cooling the solution to −30 °C did not produce any solid complex. Reducing the volume by approximately 50% and cooling similarly was unsuccessful. A small volume of the solution was evaporated to give a white power. On seeding, the cold solution with this powder and maintaining at −30 °C for 2 days gave the title compound as colorless crystals. These were filtered, washed with cold ethanol and dried at the pump. The crystals rapidly became opaque on exposure to the normal laboratory atmosphere. Yield 0.10 g (58%) Analysis Observed (required), C 36.65(36.72), H 7.25(7.19), N 5.28(5.35). Mass spectrometry (ESMS) $[M\text{-}NO_3^-]^+$ observed (calculated) 699.2403 (699.2414).

$Nd(NO_3)_3(^{t}Bu_3PO)_2{\cdot}H_2O$: $Nd(NO_3)_36H_2O$ (0.11 g 0.25 mmol) in 0.6 g ethanol and $^{t}Bu_3PO$ (0.14 g 0.64 mmol) in 0.50 g ethanol were mixed and heated to 70 °C for 30 min. Cooling the solution to −30 °C did not produce any solid complex. Reducing the volume by approximately 50% and cooling similarly was unsuccessful. A small volume of the solution was evaporated to give a lilac power. On seeding the cold solution with this powder and maintaining at −30 °C for 2 days gave the title compound as lilac crystals. These were filtered, washed with cold ethanol and dried at the pump. The crystals rapidly became opaque on exposure to the normal laboratory atmosphere. Yield 0.13 g (66%) Analysis Observed (required) C 37.03(36.98) H, 7.14(7.24), N 5.35(5.39). Mass spectrometry (ESMS) $[M\text{-}NO_3^-]^+$ observed (calculated), 704.2459 (704.2456).

$Sm(NO_3)_3(^{t}Bu_3PO)_2{\cdot}H_2O$: $Sm(NO_3)_36H_2O$ (0.10 g 0.22 mmol) in 0.5 g ethanol and $^{t}Bu_3PO$ (0.11 g 0.50 mmol) in 0.6 g ethanol were mixed and heated to 70 °C for 30 min. Cooling the solution to −30 °C for 5 days a small quantity of colorless crystals formed. These were filtered, washed with a small quantity of cold ethanol and dried at the pump to give 0.10 g (57%) colorless crystals. Analysis Observed (required) C 36.50(36.44), H 7.36(7.14), N 5.26(5.31). Mass spectrometry (ESMS) $[M\text{-}NO_3^-]^+$ observed (calculated) 712.2545 (712.2547).

$Eu(NO_3)_3(^{t}Bu_3PO)_2{\cdot}H_2O$: $Eu(NO_3)_36H_2O$ (0.09 g 0.25 mol) in 0.5 g ethanol and $^{t}Bu_3PO$ (0.15 g 0.69 mmol) in 0.6 g ethanol were mixed and heated to 70 °C for 30 min. Cooling the solution to −30 °C for 5 days a small quantity of colorless crystals formed. These were filtered, washed with a small quantity of cold ethanol and dried at the pump to give 0.13 g (66%) colorless crystals. Analysis Observed (required) C 36.59(36.36), H 7.20(7.12), N 5.28(5.30). Mass spectrometry (ESMS) $[M\text{-}NO_3^-]^+$ observed (calculated) 713.2560 (713.2562).

$Dy(NO_3)_3(^{t}Bu_3PO)_2$: $Dy(NO_3)_36H_2O$ (0.11 g 0.24 mol) in 0.3 g ethanol and $^{t}Bu_3PO$ (0.11 g 0.50 mmol) in 0.4 g ethanol were mixed and heated to 70 °C for 30 min. Cooling the solution to −30 °C for 5 days a small quantity of colorless crystals formed. These were filtered, washed with a small quantity of cold ethanol and dried at the pump to give 0.12 g (64%) colorless crystals. Analysis Observed (required) C 36.67(36.71) H 7.18(6.93) N 5.34(5.35). Mass spectrometry (ESMS) $[M\text{-}NO_3^-]^+$ observed (calculated) 724.2644 (724.2642).

$Er(NO_3)_3(^{t}Bu_3PO)_2$: $Er(NO_3)_36H_2O$ (0.10 g 0.21 mol) in 0.7 g ethanol and $^{t}Bu_3PO$ (0.13 g 0.61 mmol) in 0.5 g ethanol were mixed and heated to 70 °C for 30 min. Cooling the solution to −30 °C for 5 days pale pink crystals formed. These were filtered, washed with a small quantity of cold ethanol and dried at the pump to give 0.13 g (78%) colorless crystals. Analysis Observed (required) C 36.48(36.49) H 6.84(6.89) N 5.20(5.32). Mass spectrometry (ESMS) $[M\text{-}NO_3^-]^+$ observed (calculated) 726.2643 (726.2653).

$Lu(NO_3)_3(^{t}Bu_3PO)_2$: $Lu(NO_3)_36H_2O$ (0.10 g 0.22 mol) in 0.5 g ethanol and $^{t}Bu_3PO$ (0.13 g 0.60 mmol) in 0.6 g ethanol were mixed and heated to 70 °C for 30 min. Cooling the solution to −30 °C for 5 days colorless crystals formed. These were filtered, washed with a small quantity of cold ethanol and dried at the pump to give 0.16 g (91%) colorless crystals. Analysis Observed (required) C 36.08(36.14) H 6.94(6.82) N Mass spectrometry (ESMS) $[M\text{-}NO_3^-]^+$ observed (calculated) 735.2747 (735.2758)

Attempted synthesis of $[Ln(NO_3)_2L_3][PF_6]$ Ln = Tb, Lu

$Tb(NO_3)_36H_2O$) (0.07 g 0.15 mmol), KPF_6 (0.04 g 0.21 mmol) and $^{t}Bu_3PO$ (0.11 g 0.51 mmol) were stirred in 0.70 g CH_3CN for 16 h. Evaporation of the solvent to a small volume led to the formation of colorless crystals which were removed mechanically from the reaction mixture. Crystals selected for X-ray diffraction analysis proved to be the !:2 complex $Tb(NO_3)_3(^{t}Bu_3PO)_2 \cdot 0.5CH_3CN$ (**8**)

$Lu(NO_3)_36H_2O$ (0.07 g 0.14 mmol), KPF_6 (0.04 g 0.22 mmol) and $^{t}Bu_3PO$ 0.11 g 0.52 mmol) were stirred in 0.75 g CH_3CN for 16 h. Evaporation of the solvent to a small volume led to a white powder containing some crystalline material which were removed mechanically from the bulk. Crystals selected for X-ray analysis proved to be the previously characterized Lu complex (**7**).

dx.doi.org/10.1021/ic300142r | *Inorg. Chem.* 2012, 51, 4379−4389

■ ASSOCIATED CONTENT

Supporting Information

Additional material as noted in the text. This material is available free of charge via the Internet at http://pubs.acs.org.

■ AUTHOR INFORMATION

Corresponding Author

*E-mail: a.platt@staffs.ac.uk.

Notes

The authors declare no competing financial interest.

■ ACKNOWLEDGMENTS

We are grateful to the EPSRC for the use of the National Mass Spectrometry Service at Swansea University, the National Crystallography Service at Southampton University,[25] the solid state NMR facility at Durham University and access to the CDS facility at Daresbury. We also wish to thank Dr's Sandra Van Meuse and Robin Stein of Bruker UK Ltd for the initial solid state ^{31}P NMR spectra of $Lu(NO_3)_3L_2$.

■ REFERENCES

(1) Levason, W.; Newman, E. H.; Webster, M. *Acta Crystallogr.* **2000**, *C56*, 1308.

(2) Levason, W.; Newman, E. H.; Webster, M. *Polyhedron* **2000**, *19*, 2697.

(3) Glazier, M. J.; Levason, W.; Matthews, M. L.; Thornton, P. L.; Webster, M. *Inorg. Chim. Acta* **2004**, *357*, 1083.

(4) Bowden, A.; Platt, A. W. G.; Singh, K.; Townsend, R. *Inorg. Chim. Acta* **2010**.

(5) Massabni, A. M. G.; Gibran, N. L. R.; Serra, O. A. *Inorg. Nucl. Chem. Lett.* **1978**, *14*, 419.

(6) Manchanda, V. K.; Chander, K.; Singh, N. P.; Nair, G. M. *J. Inorg. Nucl. Chem.* **1977**, *39*, 1039.

(7) Goffart, J.; Duyckaerts, G. *Anal. Chim. Acta* **1969**, *46*, 91.

(8) Gan, X.; Duesler, E. N.; Paine, R. T.; Smith, P. H. *Inorg. Chim. Acta* **1996**, *247*, 29.

(9) Matonic, J. H.; Neu, M. P.; Enriquez, A. E.; Paine, R. T.; Scott, B. L. *J. Chem. Soc., Dalton Trans.* **2002**, 2328.

(10) A. N.Turanov, V. K.Karandashev, A.M., Fedoseev; N. I., Rodygina, V. E. Baulin Radiochem. *47*, (2005) 177.

(11) Gan, X.; Rapko, B. M.; Duesler, E. N.; Binyamin, I.; Paine, R. T.; Hay, B. P. *Polyhedropn* **2005**, *24*, 469.

(12) Paine, R. T.; Bond, E. M.; Paveen, S.; Donhart, N.; Duesler, E. N.; Smith, K. A.; Noth, H. *Inorg. Chem.* **2005**, *41*, 444.

(13) Rapko, B. M.; Duesler, E. N.; Smith, P. H.; Paine, R. T.; Ryan, R. R. *Inorg. Chem.* **1993**, *32*, 2164.

(14) Jianchen, W; Chongli, S *Solvent Extr. Ion Exch.* **2001**, *19*, 231.

(15) W.DEuan, P.Cao, Y.Zhu; J. Rare Earths, *28*, 211 (2010).

(16) Reddy, M. L. P.; Bosco Bharathi, J. R.; Peter, S.; Ramamohan, T. R. *Talanta* **1999**, *50*, 79.

(17) Hunter, Ann P.; Lees, Anthony M.J.; Platt, Andrew W.G. *Polyhedron* **2007**, *26*, 4865–4876.

(18) Bowden, A.; Horton, P. N.; Platt, A.W. G. *Inorg. Chem.* **2011**, *50*, 2553.

(19) A. F.Wells *Structural Inorganic Chemistry*, 5th Ed. Oxford University Press, Oxford, 1984.

(20) Quali, N.; Rivera, J-P; Chapon, D.; Delange, P.; Piguet, C. *Inorg. Chem.* **2004**, *43*, 1517.

(21) Geraldes, C. F. G. C.; Zhang, S.; Sherry, A. D. *Inorg. Chim. Acta* **2004**, *357*, 381.

(22) R.Hooft,. Collect: Data Collection Software; B.V. Nonius: Delft: Netherlands, 1998.

(23) Sheldrick, G.M., *SADABS*, Version 2.10, Bruker AXS Inc., Madison, Wisconsin, USA, 2003.

(24) SHELXL97 - G. Sheldrick, G. M. (**2008**), *Acta Crystallogr. A64*, 112-122.

(25) Coles, S. J.; Gale, P. A. *Chem. Sci.* **2012**, *3*, 683–689.